Titanium microbead-based porous implants: bead size controls cell response and host integration.

Engin Vrana, Agnès Dupret-Bories, Philippe Schultz, Christian Debry, Dominique Vautier, Philippe Lavalle

▶ **To cite this version:**

Engin Vrana, Agnès Dupret-Bories, Philippe Schultz, Christian Debry, Dominique Vautier, et al.. Titanium microbead-based porous implants: bead size controls cell response and host integration.. Adv Healthc Mater, 2014, 3 (1), pp.79-87. 10.1002/adhm.201200369 . inserm-00846105

HAL Id: inserm-00846105

https://inserm.hal.science/inserm-00846105

Submitted on 18 Jul 2013

HAL is a multi-disciplinary open access archive for the deposit and dissemination of scientific research documents, whether they are published or not. The documents may come from teaching and research institutions in France or abroad, or from public or private research centers.

L'archive ouverte pluridisciplinaire **HAL**, est destinée au dépôt et à la diffusion de documents scientifiques de niveau recherche, publiés ou non, émanant des établissements d'enseignement et de recherche français ou étrangers, des laboratoires publics ou privés.

Submitted to ADVANCED HEALTHCARE MATERIALS

DOI: 10.1002/adhm.((please add manuscript number))
Article type: Full Paper

Titanium Microbead-based Porous Implants: Bead Size Controls Cell Response and Host integration

Nihal Engin Vrana[1,2], Agnès Dupret-Bories[1,3], Philippe Schultz[1,3], Christian Debry[1,3], Dominique Vautier[1,2] and Philippe Lavalle[1,2]*

Dr . Nihal Engin Vrana, Dr. Dominique Vautier, Dr. Philippe Lavalle
[1]INSERM, UMR-S 1121, "Biomatériaux et Bioingénierie", 11 rue Humann, F-67085 Strasbourg Cedex, France
[2] Université de Strasbourg, Faculté de Chirurgie Dentaire, , 1 place de l'Hôpital, 67000 Strasbourg, France
E-mail: engin.vrana@protip.fr
Agnès Dupret-Bories , Dr. Philippe Schultz, Prof. Christian Debry
[1]INSERM, UMR-S 1121, "Biomatériaux et Bioingénierie", 11 rue Humann, F-67085 Strasbourg Cedex, France
[3]Hôpitaux Universitaires de Strasbourg, Service Oto-Rhino-Laryngologie, 67098 Strasbourg, France

Keywords: titanium; trachea; host integration; *in vivo*; porous implants

Abstract:

Openly porous structures in implants are desirable for better integration with the host tissue. We developed sintered microbead based titanium implants for oto-rhinolaryngology applications which create an environment where the cells can freely migrate in the areas between the micro-beads. This structure promotes fibrovascular tissue formation within the implant *in vivo*. However, this process can take several weeks and might pose risk of infection in implant areas such as trachea. In this study, we determine to what extent these events can be controlled by changing the physical environment of the implants both *in vitro* and *in vivo* as obtaining a fast integration of the implant is an important clinical goal. By cell tracking with confocal microscopy, we quantified the distribution of cells within the implants and observed that the sizecurvature of the beads and the distance between the neighboring beads significantly affect the ability of cells to develop cell-to-cell contacts and to bridge the pores. Live cell staining shows that as the bead size gets smaller (from 500 µm to 150 µm), the probability to observe cells that fill the porous areas is higher in 7 days. This also affects the initial attachment and distribution of the cells and collagen secretion by fibroblasts (higher ECM secretion in 150 µm beads over 21 days, $p<0.05$). Obtaining a fast coverage of the system also enables co-culture systems *in vitro* where, the number and the distribution of the second cell type are boosted by the presence of the first. This concept is utilized in the present study to increase the attachment of vascular endothelial cells by an initial layer of fibroblasts, which can be used for *in vitro* vascularization. By decreasing the bead diameter, the overall colonization of the implant can be significantly increased *in vivo* within 3 weeks. The effect of bead size has a similar pattern both in rats and rabbits, with faster colonization of smaller bead based structures. Using smaller beads would improve clinical outcomes as faster integration facilitates the attainment of functionality by the implant. Overall, integration of

titanium microbead based implants can be finely controlled by changing the bead size which provides an outline for integration of other implants with well defined topographical features.

1. Introduction

Titanium is a widely used biomaterial, with a long list of clinical successes in orthopedic and dental implant fields. However implant integration remains a crucial problem and to overcome this issue surface modifications have been generally used for improving cell interaction with implants. These modifications involved changing surface roughness[1], geometry[2] or applying coatings[3] such as hydroxyapatite. Recently, development of metallic foams with porosities that would allow in-growth of cells *in vivo* has become a very active area of research.[4] Utilization of metallic foams enables utilization of titanium in soft tissue applications such as tracheal replacement where mechanical properties of the structure are vital. [5] In such structures, understanding the mechanisms of the interactions of the 3D titanium structures with soft tissues is important, but it has not been as widely studied as the interaction of titanium with hard tissues.

There are three modes of integration for metallic implants: *i) in situ* where the implant interacts with the cells surrounding it upon implantation; *ii) in vivo* where the implant is first implanted in a different area (such as subcutaneous implantation) promoting the integration in a controlled way before the implant is moved to the main target area; *iii) in vitro* where the relevant cells for the target area are used before implantation. As a good integration improves the functionality of the implants and prevents infection related problems, the development of methods to obtain robust integration in a fast manner is very important for the patients' well-being. The topographical properties of the implants are o~~O~~ne of the main determinants in all these processes. Effects of topography on the behavior of cells are well-documented[6], where cells respond to topographical cues by alignment, differentiation, self assembly etc.[7] The

micro-patterning experiments showed that, the distance between the patterns and the size of the patterns are important determinants of cell behavior.[8] Recently, it was also shown that this can even be used for exclusion of microbial attachment on surfaces.[9] As some implantation areas are not sterile (such as tracheal implants) it is important that the integration of implants happens faster than possible biofilm formation by bacteria.

However there is a gray area between well controlled 2D topographical features[10] and 3D topographical structures obtained by solid freeform fabrication methods and inherently complex structure of 3D implants and scaffolds[11], where cells come across a wide array of 3D features. Micro-bead based structures falls somewhere in between random pore distribution and fabricated pores, as micro-bead assembly results in a naturally ordered structure where the bead size determines the size of the pores of the structure **(Figure 1)**. Previously, efforts to quantify the effect of 3D pore architecture on cell behavior was mostly done with opened and closed cell foams, but since lyophilization and other methods generates random pore size distributions, the results cannot be highly reproducible.[12] Actually reports have shown that in the structurally heterogeneous environment of a foam, cells behave as in 2D cultures when they interact exclusively with the surface of pore walls. But they change their behavior when the pore structure prevents them from spreading in one plane. There is also another line of study which has focused on the effect of the pore size for different cell types to determine the optimal pore sizes that promote colonization. For example it was shown that polymeric substrates with pores larger than 20 µm can have an adverse effect on vascular endothelial cell growth.[13] *In vivo* this would affect the period of invasion of the scaffold by cells. However, how highly defined 3D pores can be used to modify host integration *in vivo* has not yet been described. Also, pore size studies have focused on polymeric systems where the pore size can change with cellular activity and degradation, whereas in a metallic system it will be stable during the course of integration.

Micro-bead based structures have the advantage of a naturally open pore structure which would improve *in vivo* integration. Also, since the interconnectivity is complete, formation of pouches of bacterial growth can be prevented, which is an important advantage *in vivo* in areas where the implant is in contact with air. Previously we have used micro-bead based implants *in vivo* for tracheal replacement experiments [14] and also checked how coating them with angiogenic factors would affect their vascularization capacity.[15] We have also reported a tracheal implant development protocol in sheep where a first step was intramuscular implantation of the implant for fast colonization and the addition of anan epithelial layer ~~was added~~ on the colonized structure was the second step.[16] ~~This epithelium was crucial for the long term functionality of the implant~~. However, the integration process was rather slow and we observed through both *in vivo* and *in vitro* approaches that 500 µm beads resulted in spaces which took several weeks to become filled by newly formed tissue. We have previously shown how these structures can be improved using a composite based on association of porous titanium with a hierarchically porous system composed of polymers. This hybrid system allowed a better control of colonization and the depth movement of the cells.[17] But such control brings an additional limitation based on polymer degradation, as the pore sizes will change over time due to degradation. Thus, we hypothesized that the size of the individual micro-beads can be used to control *in vivo* implant integration process. By decreasing the bead size, the bridging between the pore areas by the cells can be increased as their ability to move between the subsequent beads is related to the distance. In order to check this hypothesis, we seeded 3T3 fibroblasts to implants having an identical total thickness but composed of different bead sizes and we monitored cell migration in z direction. We also quantified the distribution of the cells on the beads and how this was affected by the bead size. Then we validated our results with *in vivo* tests. Our previous *in vivo* experiments showed that the infiltration and filling by fibrovascular tissue might take up to 6 weeks with large beads

(500 µm in diameter), thus we checked whether there is a significant difference between different bead size samples in shorter periods of time (2-3 weeks). Another possibility of improving the integration of the implant systems is the seeding of the implants with co-culture systems ~~on them~~.[18] It has been shown previously that the co-culture of vascular endothelial cells (Human Umbilical Cord Vascular Endothelial Cells, HUVEC) with osteoblasts can induce neovessel formation and that the presence of the osteoblasts is an important promoter of this event.[19] Thus in our study, we also checked whether it would be possible to improve the attachment and proliferation of HUVEC cells over fibroblasts as an additional way to facilitate integration. By utilizing these tools it would be possible to colonize and functionalize an implant, in our case a tracheal implant, within a shorter time interval.

2. Results and Discussion

Control of the bead size should lead to discrepancies in 4 areas: *i)* migration and thus distribution of the cells in the 3D architecture; *ii)* initial cell attachment due to bead curvature; *iii)* filling of the pore volumes; *iv) in vivo* integration. For both *in vitro* and *in vivo* conditions using smaller beads led to significant differences in these properties.

2.1. 3D Distribution of Cells

We first started by observing the distribution of fibroblast cells by Scanning Electron Microscopy (SEM) and confocal microscopy. In SEM images it was possible to distinguish the difference between the level of interaction of the cells on different beads **(Figure 2)**. From large beads to small beads the cell-cell contacts between the beads changed from non-existent at 500 µm beads to extensive in 150 µm beads. In 150 µm bead samples, the areas between the beads were occasionally fully filled with cells and possibly with ECM secretions. To quantify and verify ECM presence, the secreted collagen content of the implants were

measured over time and it was found that it was significantly higher in the case of 150 µm beads at each time point during a 21 day culture period ($p<0.05$) **(Table 1)**.

In order to see the position of the cells in these structures after one week of seeding, live cells were labeled with Calcein-AM. Confocal images showed that cellular groups holding onto each other were present in the pores of small bead size samples (150 µm), this was not the case for ~~300 µm or~~ 500 µm beads where cells only stayed on the bead surfaces **(Figure 3)**. For large beads, the distance between them is high enough to prevent large scale cell to cell contact between different beads after 7 days. To understand better the extent of this difference and for determining the distribution of the cells after 1 week, z-stacks of PKH-26 labeled cell seeded implants were done. PKH-26 is an appropriate dye to monitor long term migration.[20] The intensity of the signal was converted to contour graphs by color-encoding the fluorescence signal intensity within the 3D reconstructions (Zeiss LSM Confocal Imaging Software, Germany) (**Figure 3f-h**). These graphs show that the cells' preference changes significantly with respect to bead size. For all bead sizes it was possible to see a high cell concentration at the apex, but as the bead size gets smaller cells start to follow the curvature of the beads and the distribution around the beads themselves gets higher. For 500 µm beads, cells were mostly on the top of the beads and the pore areas were nearly empty. In 300 µm beads there were hotspots for cells (higher cell density areas) -as streaks on large areas of the bead surface but the pore areas were still scarce in cells. In 150 µm bead size samples it was possible to observe from 3D stacks, cells around the central portion of the beads and also in between the beads (data not shown). So with respect to the location of the cell signal, it was seen that most of the cells in the case of large beads are located on the top of the beads, whereas in the case of the 300 µm beads, more cells could be seen in the periphery. In the case of 150 µm beads, cells were not only on the periphery of the beads but also in between the bead areas. After 7 days, there were pores in 150 µm samples that were partially covered.

2.2 Fibroblast Migration

The ability of the lamellapodia of the fibroblastic cells to assess the material surface and to determine the movement direction of the cells is a well defined process. [21] Fibroblastic cells send lamellapodia to sense the surface chemistry and topography in front of them. The decision to move forward would then depend on establishment of a strong contact with the target area. This mechanism is well known in 2D movement however in *in vivo* conditions the presence of lamellapodia is less significant. [22] The movement in a porous structure is more similar to 2D migration since the cells interact with a 2D surface and then make decisions on how to navigate in the 3D environment. This is unlike *in vivo* conditions where the cells are surrounded by ECM. Thus, while moving within porous structures, especially when the pore walls are distant to each other, a cell might not be able to extend across the walls. So as a result, in the case of micro-bead based structures, the cell would prefer to reside on the bead it has already attached to and to move on it. The previously observed results of the differential effect of pore sizes on cellular movement can be attributed to the fact that, the migration of fibroblastic cells in 3D would have a better chance of encompassing the distances between the small pores. However, classical porous systems that are created by methods like freeze-drying, freeze-extraction etc. have their pore interconnectivity *via* junctions, which can act as bottlenecks for overall cellular movement. In the open porous structure in the current study, this effect was not a problem and the differences observed were solely due to the limitations on the cellular movement.

In order to see how the microbead-defined pore structure affect 3D migration in our implants, the next step was the determination of the effect of the bead size in the movement of the cells in z direction. For this end, PKH-26 labeled cells were monitored at days 4, 7 and 14 by confocal microscopy up to the depth where no cells were observed (maximum migration

distance), to quantify overall movement of the cells **(Figure 4).** The migration pattern of the cells within the different bead size structures was significantly different ($p<0.05$ at depth 200 µm at day 4 and at depth 50 µm at day 7 and 14)-. Cells initially went deeper in larger bead size implants, but their distribution on each layer was sparser compared to smaller bead size counter parts. Surface curvature seems to be an important factor in the distribution of the cells: as the bead sizes gets larger, the surface curvature decreases (where mean curvature is 1/R) and cells experience a more planar surface where they can attach and spread easily. Whereas, as the bead size gets smaller, cells face a more curved surface which pushes them more to the central areas than the apex. Also decreasing the bead size decreases the specific surface area per bead which gives less area to cells to attach thus forcing them to move between the beads. However, this effect is compensated by the packing effect, as more small beads can be packed in a given volume, thus decreasing the contribution of the specific surface area between a 3D structure made of small beads and large beads. The sintering of the beads also creates contact points between the beads which facilitates movement of the cells. Moreover, cells tend to accumulate around these areas and then are able to cross the pores which provides them with more area to move. The cells were able to reach to the other side of the implant, as evidenced by their presence observed by confocal microscopy (Figure 4B). The decrease in the depth on day 14 was due to the amplified diffusion limitations due to the increase in overall cell number in all implants. Recently it has been shown that the responses of the cells to the geometrical obstacles are an important parameter for their behavior [23]. As fibroblastic cells tend to migrate as a whole front, when they come across an obstacle they can go through it by bridging, whereas this would not be possible for cells that migrate alone. This property of fibroblasts is an important contributor to the results observed in this study.

2.3 In vivo integration

In vivo, cellular response followed a similar pattern, regardless of the model animal, where smaller bead sizes caused increased infiltration and also maturation of the infiltrated tissue. First, subcutaneous implantation of the different bead size implants to rats was tested **(Figure 5).** The outer surfaces of the implants were more covered with tissue in the case of small bead sizes (Figure 5 A, D, G). The attachment of the implant to the subcutaneous area was not significantly different as the measurements of the mean force necessary to remove the implants during explantation with a custom-made dynamometer were not statistically significant (data not shown). At the surface, similar to the *in vitro* observations, the filling of the pores was more effective than in the small bead size samples (Figure 5 B, E, H). The SEM analysis of the cross section of the implants showed that the migration was impeded into the depth of the larger bead size implants whereas in smaller bead size implants the coverage was full (Figure 5 C, F, I). The main difference between the *in vivo* and *in vitro* observations was that *in vivo* the colonization of the middle implant zone was faster due to the increased speed of migration for all implants, particularly for 300 µm bead implants. Distribution of the cells proved that the implant shape related differences in cell behavior persist under *in vivo* conditions and by controlling the bead size, the rate of integration of the implant can be easily controlled. Another discrepancy observed was at certain areas 300 µm bead implants had higher infiltration, due to the high compaction of 150 µm beads in some areas. This effect can be rectified by using a mixture of different bead size to control the compaction of the beads, *i.e.* the pore size.

All implants were mostly covered, but the vascularization of the smaller bead size implants was better. In rabbits, angiogenesis was even more apparent in smaller bead sizes as well developed veins and arteries were visible on the implants **(Figure 6).**

Histological analysis of the samples explanted from rabbits after subcutaneous implantations showed that the bead size also has a qualitative effect on the integration process. For 150 µm

and 300 µm samples a maturing connective tissue was clearly present between the beads deep into the scaffolds (the extent of the tissue was higher for 150 µm samples) whereas only a fibrous tissue coverage was present in the case of 500 µm samples (Figure 6). There is a clear correlation between our *in vitro* observations and the integration process monitored *in vivo*. This will be especially beneficial for having control over initial inflammatory response as the interaction of macrophages with implant surfaces is an important determinant of successful implant integration.[24]

2.4 Co-culture conditions

To assess whether the cell behavior discrepancies observed on different bead size samples is cell type dependent, we have quantified the cell initial attachment and proliferation for 3T3 fibroblasts and HUVEC (Human Umbilical Vein endothelial cells) both alone and in co-culture **(Figure 7)**. As the cell suspension goes through the implant, the 500 µm beads provide a large surface for cells to attach and to form a layer on them. Due to this, the initial attachment quantified as the cell number 24 h post-seeding on the 500 µm bead implants was the highest (Figure 7A). This tendency was similar for both 3T3 and HUVEC cells. However, this does not directly result in a higher proliferation in long term (Figure 7B). The differences in proliferation were not always statistically significant ($p>0.05$) and by 14 days the cell numbers were at comparable levels for all bead sizes. Thus the differences in the integration are not related to the differential cell numbers. Cell growth was not the main driving force behind the differences observed in the cell distribution as the cell numbers are similar for all bead sizes.

For both cell types tested, the trend was similar in the case of initial attachment where larger bead sizes caused higher attachment of cells overall. The size of the beads do not influence cell proliferation in the case of 3D structures presented in this work, but for single alginate

microcarrier beads it has been recently shown that an inverse relationship between the bead size and cell proliferation was observed. [25] However this was done under bioreactor conditions, where also the shear stress can be a major affecting factor. In the current work, the differences seen in the mode of integration is due to the cell distribution and their differential ability to interact on beads with different sizes. With smaller beads, cells on adjacent beads can form contacts and move between the beads, which enable an increased filling of the structure without a strong increase in cell proliferation.

Previous works concerning the relation between pore size and cell behavior used the pore size as the main parameter [26] while the geometrical structure induced by the pores is generally not considered. The importance of the distinction between the pore architecture and porosity has been recently shown with the behaviour of mesenchymal stem cells on CAD designed gyroid shaped PLLA scaffold versus salt leached scaffolds of comparable porosity. The gyroid structure by virtue of having an equal interconnection at each point had better cell distribution compared to the salt leached counterpart.-[27]

The cell movement largely depends on the geometry and the surface properties such as charge [28] which can be tuned by applying certain coating procedures, as demonstrated previously for anti-inflammatory response on titanium surfaces.[29] Another possibility is to use a "precursor" layer of fibroblasts as a coating to improve the behavior of another cell type. This concept has been used with vascular endothelial cells, which are important actors in the cases where *in vitro* vascularization is necessary.[30] By themselves, HUVEC cells were able to attach titanium implants but their proliferation and ability to cover titanium surfaces was quite low (Figure 7D). However when they are seeded onto fibroblast seeded implants (Figure 7E), this caused an increase in their distribution even for the 500 µm bead implants. Moreover, their ability to bridge the beads is also increased as evidenced by PKH-26 stained samples (Figure 7 G-H). Large areas were covered under these conditions and sprouting structures were

observed showing that a natural coating of the surface by cells can act as a promoter of a secondary cell attachment. It has been shown previously that endothelial cells sprout within hydrogel environments.[31] In the present case, the contacts and the secretions of the underlying fibroblasts provided these cues. The functionality of HUVEC cells was checked with NO secretion levels which were similar for all bead size implants and not detectable where only fibroblasts were seeded on the samples (data not shown). The ability of fibroblast layers to support HUVEC cells were also validated by 2D experiments of pre-seeded fibroblasts, which showed that a 7 day culture period provides a better surface for cell attachment. As controlling bead size affects fibroblast population, together with the effect of fibroblast presence on HUVEC cells, an exponential decrease in the integration period can be foreseen by using this strategy mix.

3. Conclusion

The ability to control the colonization by changing the bead size of the building blocks is an example of how modular approaches in biomedical field can be used for improving *in vivo* outcomes. The current study shows that by arranging the architecture of a porous structure, it is possible to influence and facilitate cellular migration and host integration. The ability to cover open volumes by cells *in vitro* and *in vivo* will enable faster formation of functional tissue. By controlling the interaction of the cells with single beads it might also be possible to obtain better osteoblast infiltration for bone applications or better periodontal closure in dental applications. We have been working on demonstrating that the surfaces obtained after subcutaneous implantation are suitable for promoting respiratory epithelium [32], which would improve dramatically the clinical success of these implants as tracheal substitutes. Our current work focuses on utilization of this system for tissue substitution, particularly for full tracheal replacement in rabbits.

4. Experimental Section

Implant Production: Medical grade pure titanium beads with different granulometry ranges were seperated into 3 groups (150-250 µm, 300-400 µm and 400-500 µm respectively) and then in molds were meshed together with an electrical arc. After sintering, the final implants which are 1.5 mm thick were cleaned in acetone in an ultrasonicated bath and sterilized first with UV and then 70% ethanol prior to in vitro cell culture experiments and implantation

Cell Culture

Fibroblast Cell culture: NIH-3T3 fibroblasts were cultured in RPMI 1640 medium (Gibco, USA) with 10% Foetal bovine serum and Pen/strep. The implants were sterilized by 70% Ethanol for 2 hours and then washed with sterile PBS and placed into cell culture plates. Confluent cells were removed with triple express enzyme cocktail (Invitrogen, USA). Total cell number was determined with a a haemocytometer and the cells were marked with PKH26 fluorescent red cell linker (Sigma Aldrich) according to the providers instructions. Marked cells were seeded onto the implants at a concentration of 2 x 10^6 cells/implant. Medium was changed twice a day and at day 7, samples were fixed with 4% Glutaraldehyde and gold coated and observed with SEM (n≥3). For each bead size sample at day 7, cells were- labeled with Calcein-AM used as per instructions of the provider (Invitrogen, USA). Briefly the culture was then supplemented with Calcein-AM containing medium with the final concentration of Calcein-AM as 5 µM. Then the cells were incubated at 37 °C for 1 hour washed with medium and PBS and fixed with 3.7% paraformaldehyde. The cell-cell interactions of Calcein-AM labeled cells were checked with confocal microscopy (Zeiss LSM 510, Germany) in order to see the bridging of the pores by multiple cells. For the migration of the cells fibrob~~a~~lasts were labelled with PKH-26 and the z-stacks of the samples from both bottom and top were taken at days 4,7 and 14. For each sample at least 26 stacks were

analyzed by Image J software (NIH, USA) between the top layer (where the cells were seeded) and the layer where when the signal is lost. Cell number at each stack was determined. To determine cell proliferation, samples were seeded with 1 x 10^5 cells/implant and then cell numbers were determined over a course of 2 weeks with TOX8 (Sigma Aldrich) assay. this is a Resazurin based assay, where cell number can be inferred from the decrease in the absorption of the dye in 600 nm due to metabolic activity. The level of cell attachment was determined with atest at 24 h time point. –The test was done on samples up to 14 days with a 2 hours of incubation and with readings at reference wavelength of 690 nm. As positive control TCPS was used (n≥6).

HUVEC culture and co-culture experiments: Human Umbilical Vein Endothelial cells (HUVEC, PromoCell, Germany) were used at passage 4-5 for all experiments. Cell culture was done with Endothelial Cell Growth Medium (PromoCell, Germany) with supplement mix and 1% Pen/Strep. For Co-culture experiments, fibrobalst seeded samples were seeded with 1 x 10^5 HUVEC at day 7 and the total medium is changed to endothelial growth medium. Seperate experiments with the fibroblasts showed that this medium does not cause death of t he fibroblasts but stops their growth. To differentiate between the fibroblasts and HUVEC cells, HUVEC cells were marked with PKH-26 and after 7 days they were observe with both confocal microscopy and Scanning Electron Microscope (SEM, Hitachi TM100) after fixation.

Collagen Determination: The amount of collagen over a cours-e of 3 weeks was determined by Chondrex Semi-Quantitative Collagen Micro-assay kit (Chondrex, USA) as per providers instructions. Briefly, the samples were incubated in Kit dye solution for 30 minutes and after washing with PBS, the dye that bind to collagen was extracted with extraction solution and the absorption of the solution was measured at 540 nm and 605 nm (Multi–plate reader

Multiskan EX from Thermo Scientific, France). The amount of collagen (in µg) was calculated from the following equation:

Collagen amount = $[OD_{540nm}-(OD_{605}*0.291)]/37.8*1000$

In vivo experiments

Rats: After Wistar rats (n≥6) were anesthetized with intraperitoneal administration of ketamine (20 mg/kg, Ketamine 500®; Virbac France) in combination with midazolam (10 mg/kg, Mydazolam®; Mylan, France) and atropine (0.25 mg/kg). They were placed in the prone position [14]. Surgical procedures were performed under standard aseptic conditions. A single dorsal incision was made in the lower back to expose the paraspinal muscles.

Four titanium plates with same porosimetry were implanted into sockets made within the paraspinal muscle (2 on the right side and 2 on the left side of the incision). Each plate was sutured to the muscles with one stitch (vicryl 4.0). After rinsing with saline, the wound was closed in layers. Two weeks after surgery, the animals were euthanized with an overdose of sodium thiopenthal (100mg/kg). The implants with surrounding tissues were excised.

Rabbits: The surgery was performed under general anesthesia. Anesthesia was induced by intramuscular administration of ketamine (30 mg/kg) in combination with midazolam (0.2 mg/kg) and xylazine (3mg/kg) and assisted ventilation (O_2:1 l/min) [32].

The operation was performed under sterile conditions. With the animal (New Zealand White Rabbits) in the prone position a single dorsal incision was performed in the lower back to expose the paraspinal muscles.

Four titanium plates with different porosimetry were implanted into sockets made within the paraspinal muscle (2 on the right side and 2 on the left side of the incision). Each plate was sutured to the muscles with one stitch (vicryl 3.0). After rinsing with saline, the wound was closed in layers. Postoperative analgesia was maintained by fentanyl patch (3 µg, Fentanyl-

Mepha®;Mepha Pharma, Austria) for three days. Two weeks after the rabbit was euthanized with an intravenous overdosed of sodium pentobarbital (120 mg/kg) after intramuscular administration of anesthesia (same protocol previously described). The implants with surrounding tissues were excised.

Explantation and Histology: After 3 weeks the subcutaneous implants were explanted after intramuscular administration of anesthesia. Sectioning of the impalnts and haemotoxylin and eosin staining was done as reported previously [14]. Histological analyses were performed at the IMM (Institut Mutualiste Monsouris, Paris, France), where the blinded analyses were performed by two pathologists not involved in the project.

Statistical analysis: Statistical significance between different bead sizes was tested with one-way ANOVA test together with Tukey's honest significant difference test for each time point (Significance limit $p \leq 0.05$).

Supporting Information

Supporting Information is available online from the Wiley Online Library or from the author.

Acknowledgements

Authors would like to thank Dr. A. Walder from ONERA, (Office National d'Etudes et de Recherche Aérospatiale) for providing titanium samples. We thank Pr. J.-H. Lignot from IPHC-DEPE-CNRS (Strasbourg) for scanning electron microscopy and Dr. G. Prevost from Institute of Bacteriology (University of Strasbourg) for his help with animal experimentation. We acknowledge the PMNA (Pôle Matériaux et Nanosciences d'Alsace), Région Alsace,

Formatted: Font: Not Bold

Communauté Urbaine de Strasbourg and EuroTransBio "BiMoT" project (ETB-2012-32) for financial contribution.

Received: ((will be filled in by the editorial staff))
Revised: ((will be filled in by the editorial staff))
Published online: ((will be filled in by the editorial staff))

References:

[1] B. Baharloo, M. Textor, D. M. Brunette, *J. Biomed. Mater. Res., Part A*. **2005**, *74A*, 12.

[2] C. Matschegewski, S. Staehlke, R. Loeffler, R. Lange, F. Chai, D. P. Kern, U. Beck, B. J. Nebe, *Biomaterials* **2010**, *31*, 5729.

[3] S. Werner, O. Huck, B. Frisch, D. Vautier, R. Elkaim, J. C. Voegel, G. Brunel, H. Tenenbaum, *Biomaterials* **2009**, *30*, 2291.

[4] G. Ryan, A. Pandit, D. P. Apatsidis, *Biomaterials* **2006**, *27*, 2651.

[5] L. M. Janssen, G. van Osch, J. P. Li, N. Kops, K. de Groot, L. Feenstra, J. A. U. Hardillo, *J. Tissue Eng. Regener. Med.* **2010**, *4*, 395.

[6] K. Anselme, P. Davidson, A. M. Popa, M. Giazzon, M. Liley, L. Ploux, *Acta Biomater.* **2010**, *6*, 3824.

[7] J. N. H. Shepherd, S. T. Parker, R. F. Shepherd, M. U. Gillette, J. A. Lewis, R. G. Nuzzo, *Adv. Funct. Mater.* **2011**, *21*, 47.

[8] E. Vrana, N. Builles, M. Hindie, O. Damour, A. Aydinli, V. Hasirci, *J. Biomed. Mater. Res., Part A.* **2008**, *84A*, 454.

[9] Y. Wang, G. Subbiahdoss, J. Swartjes, H. C. van der Mei, H. J. Busscher, M. Libera, *Adv. Funct. Mater.* **2011**, *20*, 3916.

[10] M. M. Stevens, J. H. George, *Science* **2005**, *310*, 1135.

[11] V. Karageorgiou, D. Kaplan, *Biomaterials* **2005**, *26*, 5474.

[12] Y. Huang, M. Siewe, S. V. Madilhally, *Biotechnol. Bioeng.* **2006**, *93*, 64.

[13] D. Narayan, S. S. Venkatraman, *J. Biomed. Mater. Res., Part A.* **2008**, *87A*, 710.

[14] P. Schultz, D. Vautier, A. Charpiot, P. Lavalle, C. Debry, *Arch. Oto-Rhino-Laryngol.* **2007**, *264*, 433.

[15] S. Muller, G. Koenig, A. Charpiot, C. Debry, J. C. Voegel, P. Lavalle, D. Vautier, *Adv. Funct. Mater.* **2008**, *18*, 1767.

[16] A. Dupret-Bories, P. Schultz, N. E. Vrana, P. Lavalle, D. Vautier, C. Debry, *J. Rehabil. Res. Dev.* **2011**, *48*, 851.

[17] N. E. Vrana, A. Dupret, C. Coraux, D. Vautier, C. Debry, P. Lavalle, *PLoS One* **2011**, *6*.

[18] C. J. Kirkpatrick, S. Fuchs, R. E. Unger, *Adv. Drug Delivery Rev.* **2011**, *63*, 291.

[19] A. Hofmann, U. Ritz, S. Verrier, D. Eglin, M. Alini, S. Fuchs, C. J. Kirkpatrick, P. M. Rommens, *Biomaterials* **2008**, *29*, 4217.

[20] W. Christian, T. S. Johnson, T. J. Gill, *J Biomed Sci Eng* **2008**, *1*, 163.

[21] G. Albrechtbuehler, *J. Cell Biol.* **1976**, *69*, 275.

[22] J. S. Harunaga, K. M. Yamada, *Matrix Biol.*, **2011**,*30*,363.

[23] R. J. Mills, J. E. Frith, J. E. Hudson, J. J. Cooper-White, *Tissue Eng., Part C* **2011**, *17*, 999.

[24] S. Gordon, *Nat. Rev. Immunol.* **2003**, *3*, 23.

[25] J. J. Schmidt, J. Jeong, H. Kong, *Tissue Eng. Part A* **2011**, *17*, 2687.

[26] F. J. O'Brien, B. A. Harley, I. V. Yannas, L. J. Gibson, *Biomaterials* **2005**, *26*, 433.

[27] F. P. W. Melchels, A. M. C. Barradas, C. A. van Blitterswijk, J. de Boer, J. Feijen, D. W. Grijpma, *Acta Biomater.* **2010**, *6*, 4208.

[28] D. Vautier, J. Hemmerle, C. Vodouhe, G. Koenig, L. Richert, C. Picart, J. C. Voegel, C. Debry, J. Chluba, J. Ogier, *Cell Motil. Cytoskeleton* **2003**, *56*, 147.

[29] P. Schultz, D. Vautier, L. Richert, N. Jessel, Y. Haikel, P. Schaaf, J. C. Voegel, J. Ogier, C. Debry, *Biomaterials* **2005**, *26*, 2621.

[30] A. Alajati, A. M. Laib, H. Weber, A. M. Boos, A. Bartol, K. Ikenberg, T. Korff, H. Zentgraf, C. Obodozie, R. Graeser, S. Christian, G. Finkenzeller, G. B. Stark, M. Heroult, H. G. Augustin, *Nat. Methods* **2008**, *5*, 439.

[31] K. T. Morin, R. T. Tranquillo, *Biomaterials* **2011**, *32*, 6111.

[32] N. E. Vrana, A. Dupret-Bories, C. Bach, C. Chaubaroux, C. Coraux, D. Vautier, F. Boulmedais, Y. Haikel, C. Debry, M.-H. Metz-Boutigue, P. Lavalle, *Biotechnol. Bioeng.* **2012**, *8*, 2134.

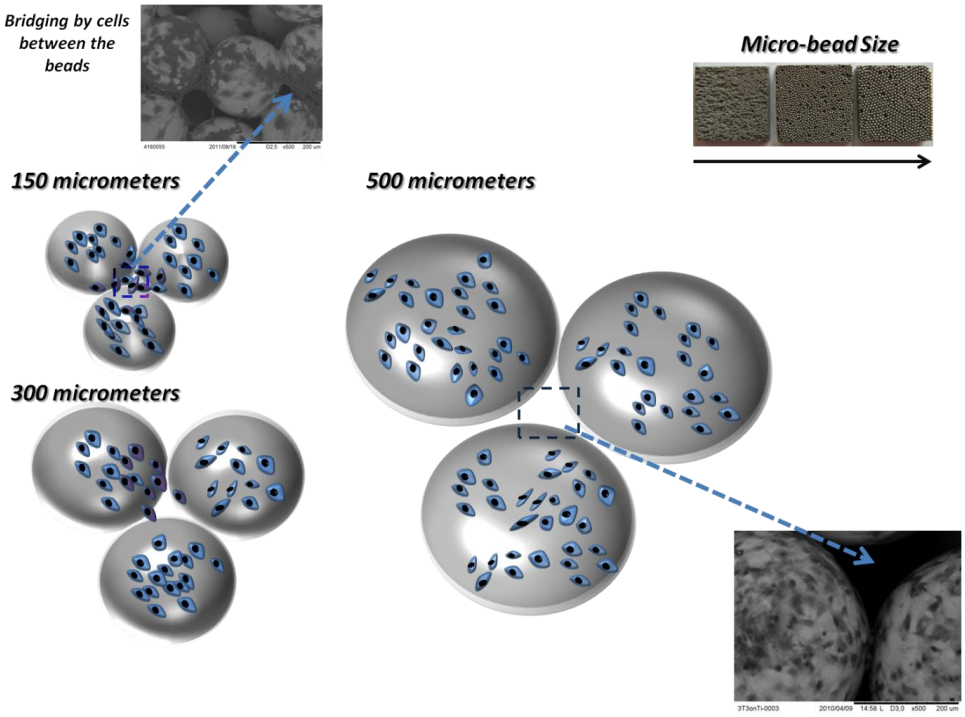

Figure 1. Production of implants with different granulometry. It is possible to obtain with different titanium microbeads robust implants with a similar total porosity. Due to the differences in the pore sizes, the attachment and distribution of the cells is distinctly different for different bead size implants, which can be useful for controlling integration period. Inset: the Macroscopic view of sample subcutaneous implants with different bead sizes (150, 300 and 500 µm in diameter, respectively).

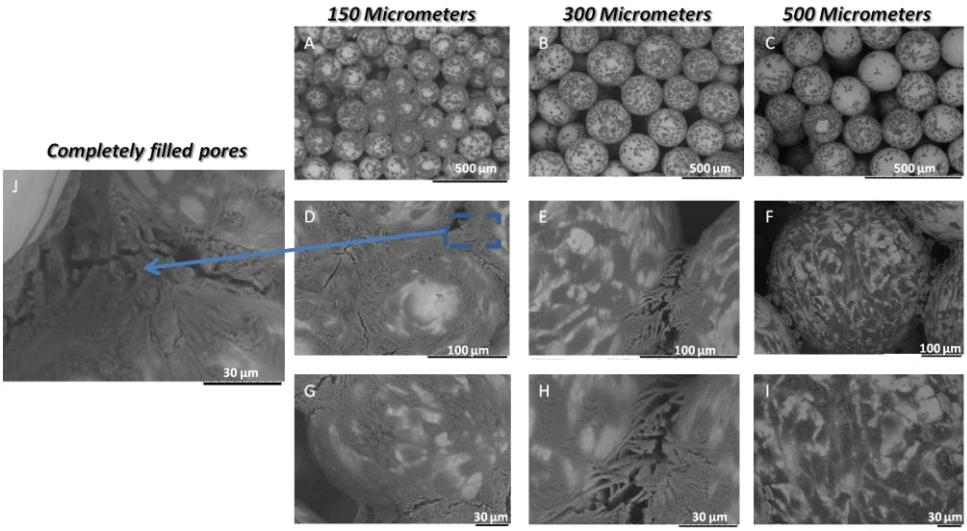

Figure 2. SEM images of fibroblasts after 7 days of culture on different bead sizes. For 150 µm bead samples (A, D, G and J), after 7 days the pores where totally or partially covered by the cells. The dense nature of these areas suggests presence of ECM, which is quantified to be higher in the case of 150 µm beads (Table 1). Bead to bead cell contacts were available but much less in the case of 300 µm beads (B, E, H), whereas for 500 µm beads, they were nearly non-existent and cells covered preferentially on the surface of the beads (C, F, I) particularly the top part.

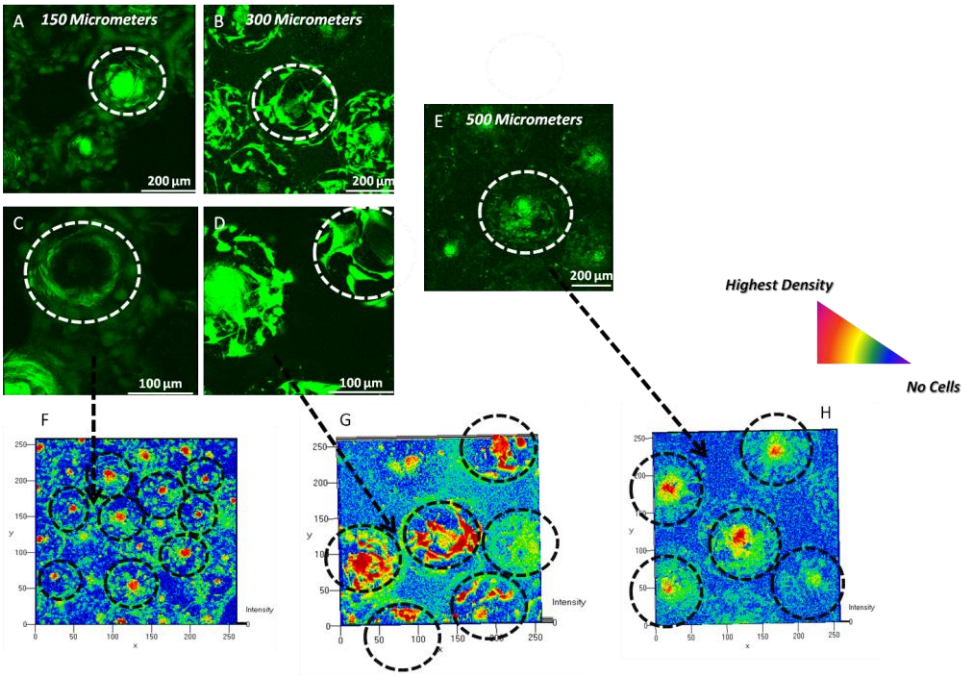

Figure 3. A-E) Calcein-AM staining of the fibroblasts on different bead sizes after 7 days, the areas between the beads is bridged by groups of cells in the case of 150 µm beads, whereas similar bridging is scarce in the case of 300 µm beads. Cells were solely present on the beads for 500 µm samples. F-H) Contour graphs of PKH-26 labelled cells after 7 days, Red color means high number of cells, blue color means absence of cells and green color means intermediate level. Cell presence in the pores distinctly decreases from small beads to larger beads also distribution of the cells shows distinct differences, a more diffuse hot spot regions for 300 µm beads, concentration on the apex for 500 µm beads and a more equilibrated distribution for 150 µm beads.

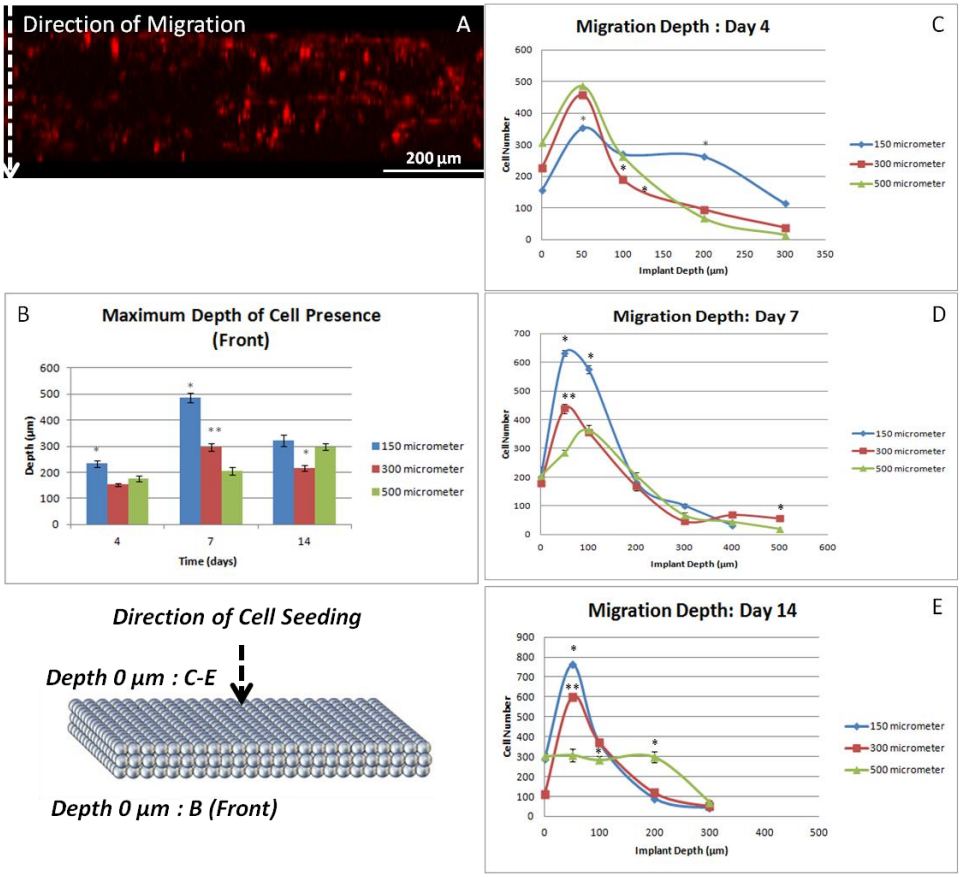

Figure 4. Fibroblast migration through the implants with different bead sizes. A) Representative cross-section of the migration samples. B) The maximum depth where cells were detected to the opposite face to where the cells were seeded (front). Depth 0 denotes the point where the implants touch the transwell surface where cells are seeded at the other side (which would denote 1500 µm depth). For day 4 and day 7 depth of reach was significantly higher for 150 µm samples ($p<0.05$) ($n\geq3$, error bars denote standard deviation. * signifies statistical significance with the marked sample with the others and ** signifies statistically significant difference between all three samples) C-E) z- direction distribution of cells on different bead size implants over course of two weeks with respect to their movement from their seeding position (Denoted as 0 depth). Initially, on 150 micrometer bead samples, cells

were able to settle deeper, whereas over the course of migration, thick layers of cells closer to the seeding surface prevailed. A similar, but less pronounced behavior was observed for 300 µm bead samples, whereas for 500 µm bead samples initial movement was mostly limited to first 100 µm and then a homogenous distribution of the cells close to the implant surface was observed after 14 days. Cell number is calculated with an average of 26 stacks and image sizes of 920 x 920 μm^2 (n=8 for each time point, with 3 images per stack for each sample).

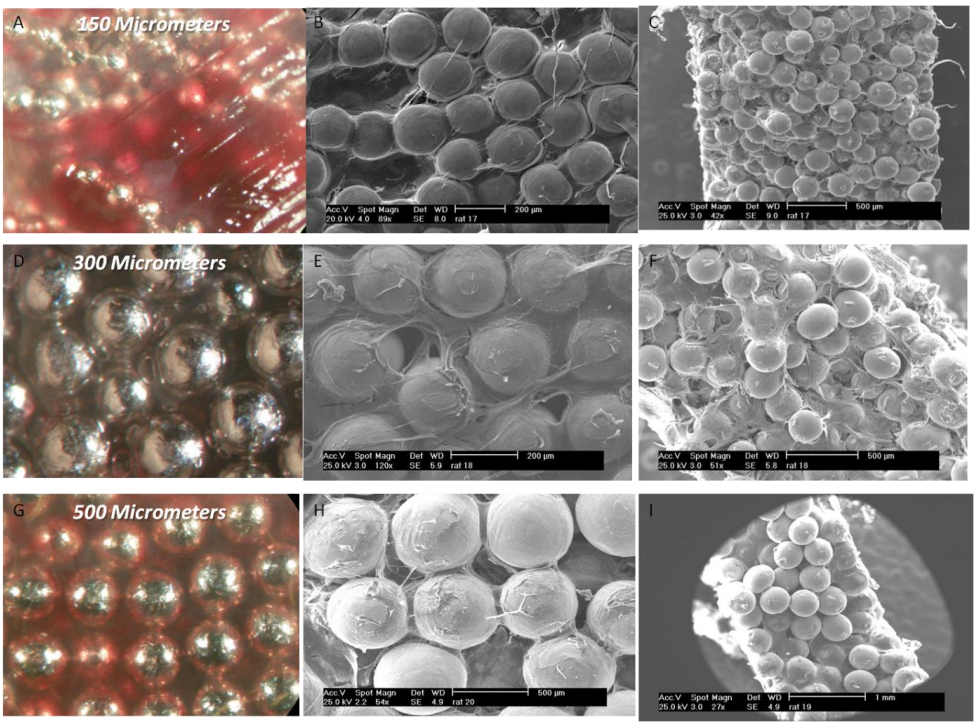

Figure 5. Subcutaneous implantation of the different bead size implants to rats for a 3 week period. A, D, G) Macroscopic view of the freshly explanted implants, 150, 300 and 500 µm bead size respectively. B, E, H) Surface of the explanted implants. The coverage by the cells decreases for the 500 µm bead size implants. Unlike *in vitro* conditions cells tend to move deeper into the implants. C, F, I) SEM images of the cross-section of the explanted implants;

colonization of the core of the implant decreases as the bead size increases. Large empty areas were visible in the case of 500 µm bead size.

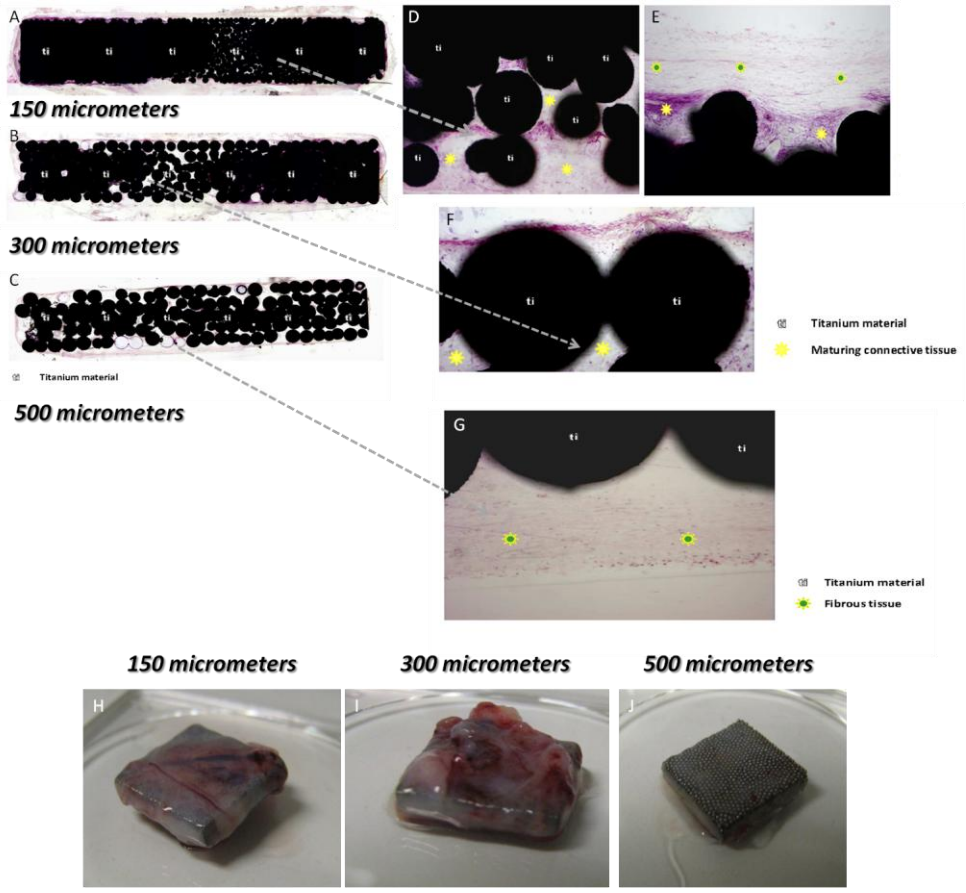

Figure 6. H&E staining of implants with different bead sizes after subcutaneous implantation in rabbits: A), D), E) 150 µm; B), F) 300 µm and C), G) 500 µm. A maturing connective tissue penetrated into the pore areas for 150 µm and 300 µm samples, whereas the in-growth and tissue maturation was lower when the bead size was bigger. H-J) Explants of different bead sizes from rabbits. The level of tissue integration vascularization was higher on 150 µm and 300 µm bead samples.

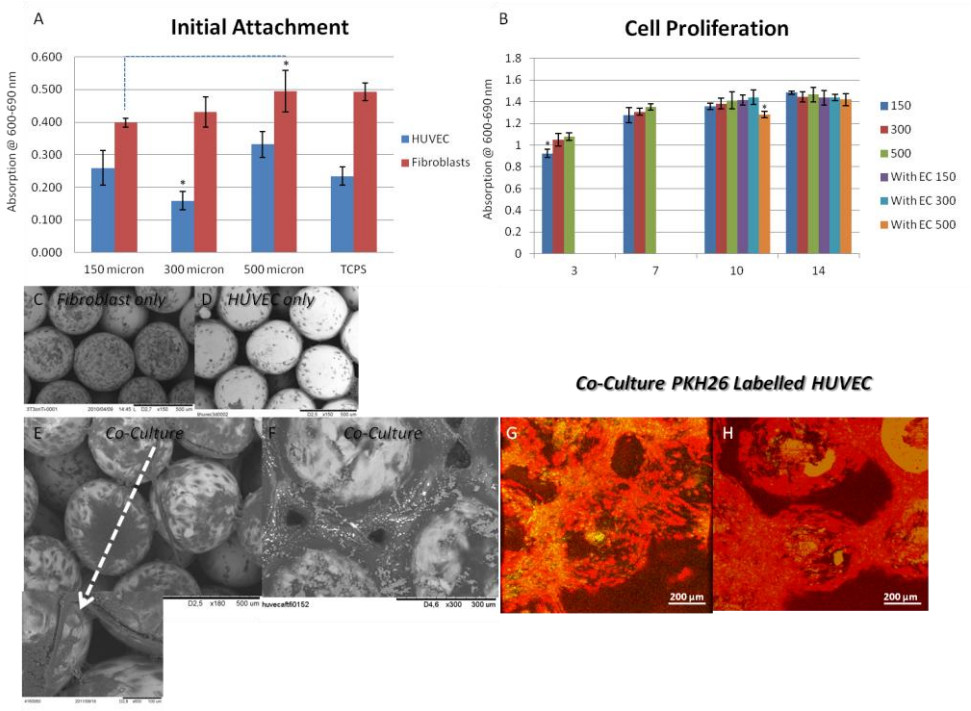

Figure 7. Fibroblast cell attachment and proliferation on different bead sizes and co-culture with vascular endothelial cells. A) Cell attachment was higher on bigger bead sizes. B) Cell proliferation followed a similar rate for all bead sizes, which shows that the difference in integration is independent of cell growth (bead size was 500 µm, EC denotes endothelial cell presence.). SEM images of : C) Only fibroblasts; D) Only HUVEC cells after 7 days; E) w~~W~~hen fibroblasts and HUVEC cells were co-cultured, surface coverage dramatically improved after 7 days; ~~-~~ F) a~~A~~fter 7 days of co-culture some pores were totally covered. G-H)

Confocal images showed that PKH-26 labelled HUVEC cells contributed to the coverage more when they are co-cultured.

Table 1. Secreted Collagen amounts by fibroblasts seeded on different bead size samples. Mean values of n≥3 samples and standard deviations

Collagen Amount [µg]	150 µm	300 µm	500 µm
Day 7	6.56±0.60	5.97±0.02	4.74±0.27
Day 14	15.72±0.65	7.40±0.44	9.74±0.30
Day 21	23.37±1.03	16.81±0.53	15.77±0.37

Keyword titanium; trachea; host integration; *in vivo*; porous implants

Nihal Engin Vrana, Agnès Dupret-Bories, Philippe Schultz, Christian Debry, Dominique Vautier and Philippe Lavalle

Titanium Microbead-based Porous Implants: Bead Size Controls Cell Response and Host integration

Micro-bead based porous titanium implants with different granulometries significantly affect cell behavior both *in vitro* and *in vivo*. By using smaller micro-bead, faster filling of the pores is achieved *in vitro* and also implants with smaller bead size integrated faster with the host in rat and rabbit models. Utilization of such physical features for controlling implant integration can ensure fast, robust attachment for many applications such as dental, tracheal and hip implants. The image shows the bridging behavior by labeled fibroblasts between adjacent beads (Image Colored for clarity: Green (Cells), Red(Titanium beads)).

ToC figure

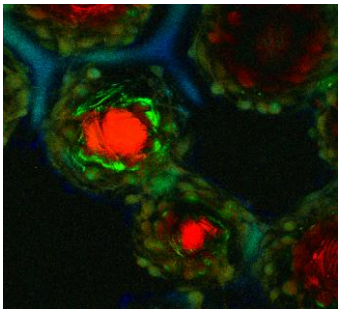

((Supporting Information can be included here using this template))

Copyright WILEY-VCH Verlag GmbH & Co. KGaA, 69469 Weinheim, Germany, 2010.